Graphene with Multiscale Synergistic Optimization: Achieving Superior Cross-Band Electromagnetic Wave Absorption Performance

Pei Liu[a,b], Kai Xu[a], Qingqing Gao[a], Yinxu Ni[a], Zhilei Hao[a], Changtian Zhu[a], Jin Chen[a], Guohui Tang[a], Zixuan Ding[a], Zhixiang Li[a], Gaojie Xu[a], Hui Zhang*[c], Fenghua Liu*[a,b]

[a] Ningbo Institute of Materials Technology & Engineering, Chinese Academy of Sciences, Ningbo 315201, PR China

[b] University of Chinese Academy of Sciences, Beijing 100049, PR China

[c] School of Materials Science and Engineering, Anhui University, Hefei 230601, PR China.

* Corresponding author.
E-mail address: lfh@nimte.ac.cn, zhhui@ahu.edu.cn.

Tab. S1 The proportion of elements obtained from XPS analysis of graphite oxide and RGO at different temperatures.

the proportion of elements (%)	C	O	S
Graphite Oxide	72.26	25.26	1.89
RGO600	93.89	6.11	0
RGO800	96.90	3.10	0
RGO1000	97.81	2.19	0

Tab. S2 Tensile properties of LCE and RGO/LCE composites.

Samples	tensile strength (MPa)	Young's modulus (MPa)	fracture elongation (%)
LCE	0.205±0.05	0.55±0.15	75.17±1.80
RGO/LCE	0.31±0.03	1.49±0.36	74.27±1.85

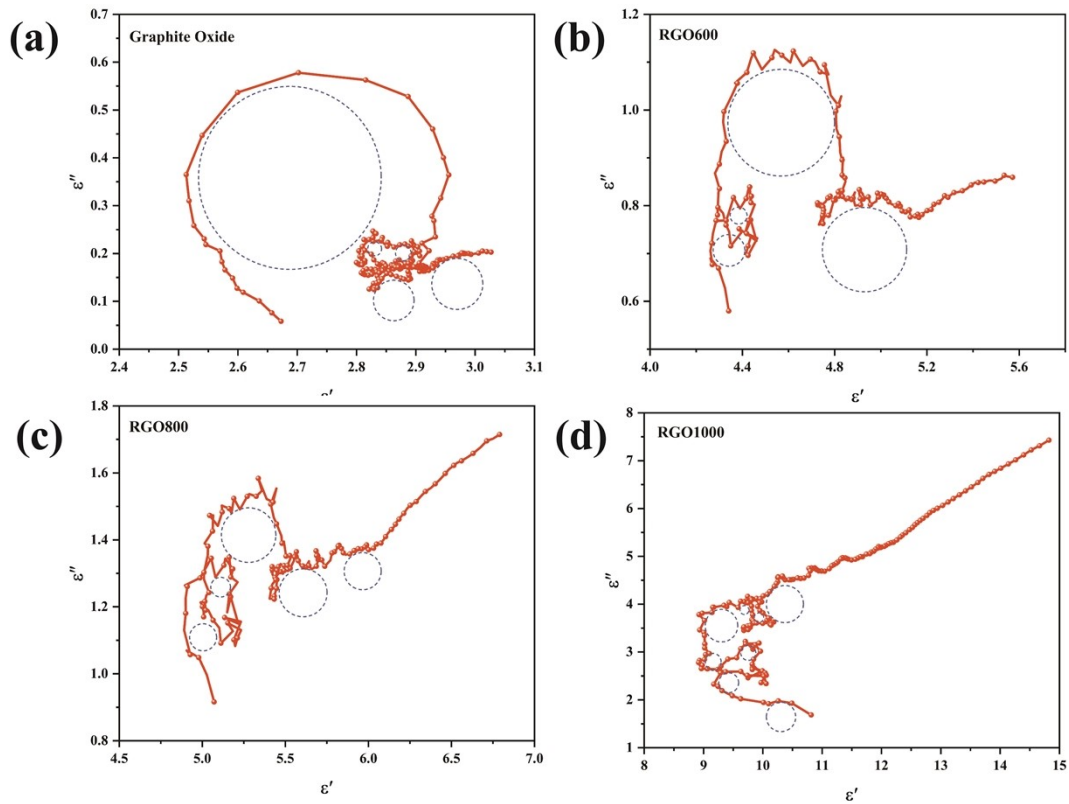Fig. S1 The ε'-ε'' curves of graphite oxide and RGO at different temperature.

The attenuation constant (α) equation was used to further analyze the wave-absorbing properties

of RGO at different reduction temperatures.

$$\alpha = \frac{\sqrt{2}\pi f}{c}\sqrt{\left(\mu''\varepsilon'' - \mu'\varepsilon'\right) + \sqrt{(\mu''\varepsilon' - \mu'\varepsilon')^2 + (\mu'\varepsilon'' + \mu''\varepsilon')^2}}$$
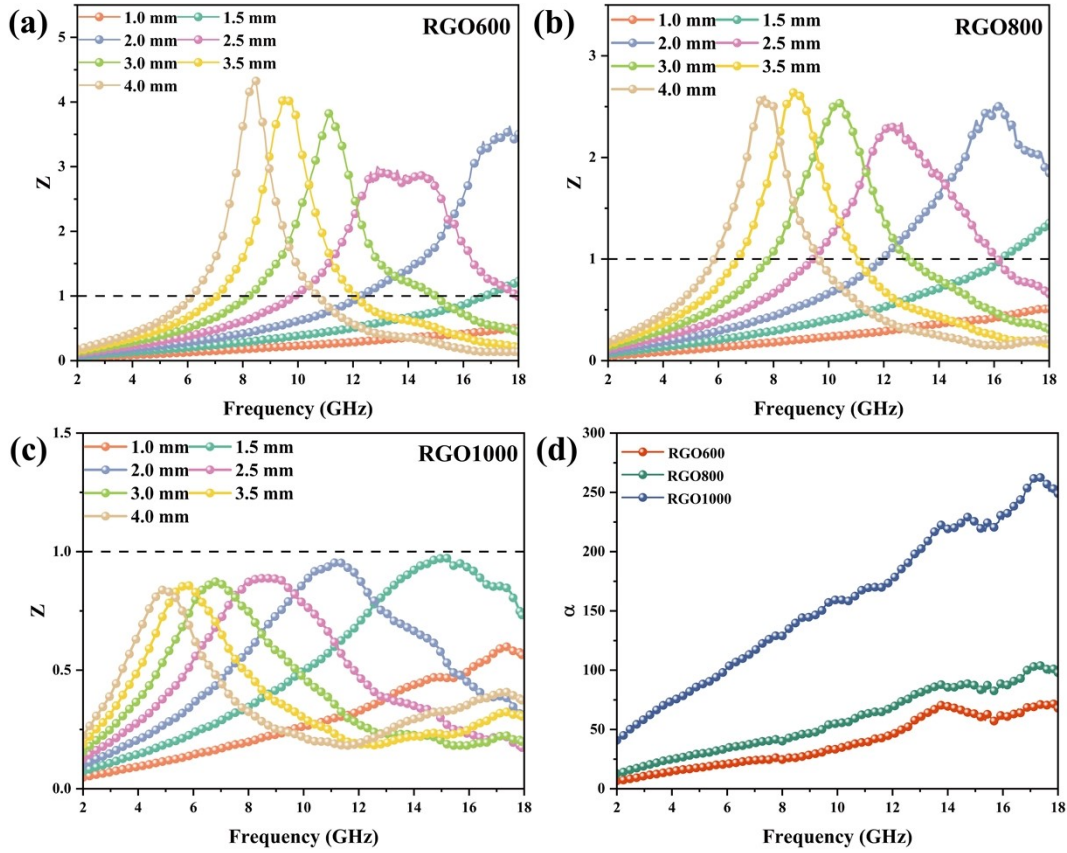

Fig. S2. (a-c) Impedance matching values (Z) and (d) attenuation constants (α) of RGO for different reduction temperatures.
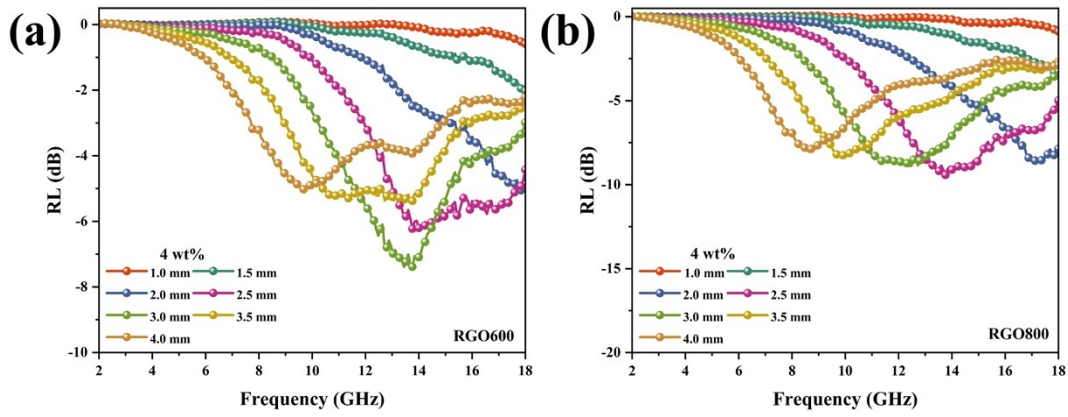
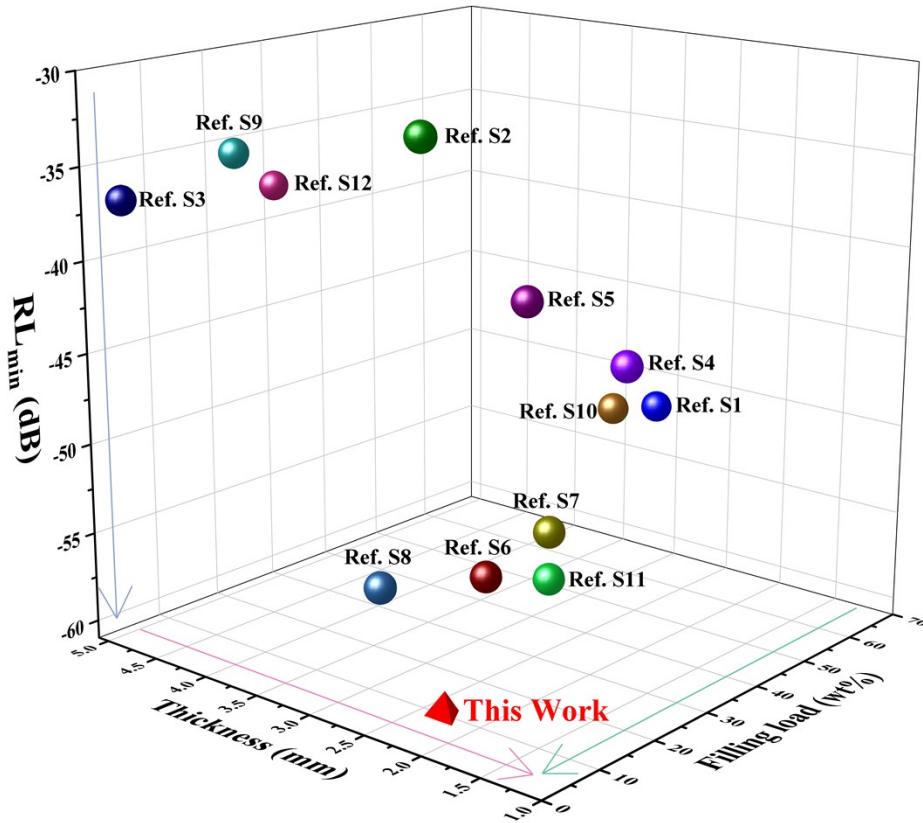Fig. S3. The RL of (a) RGO600 and (b) RGO800.

Fig. S4. Comparison of RGO bilayer honeycomb structures and related literature.

Tab. S3 Comparison of EMW absorption properties of RGO double-layer honeycomb structure in this work and graphene-based composites reported in the literature (2-18 GHz).

| Absorber	Thickness (mm)	Filling load (wt%)	RL_{min} (dB)
3D printed RGO double layer honeycomb structure (This work)	2.0	4	-59.2
3D printed RGO/SCI double-layer woodpile structure[1]	3.2	70	-52.2
3D rGO-MoS$_2$[2]	2.5	10	-31.57
RGO/nonwoven fabric filled honeycomb structure[3]	5	4.7	-37
CNT-rGO-Co/Ni-MOF[4]	1.5	25	-43
Fe$_3$C@NC/G[5]	2.1	20	-40.05
Cu/expanded Graphite composites[6]	2.2	15	-54
3D NrGO/Co–MnO aerogels[7]	1.9	20	-51.7
Fe/RGO composites[8]	2.45	2	-53.38
Graphene/g-C$_3$N$_4$[9]	4.5	15	-34.69
NbS$_2$/PrGO hybrids[10]	2.28	40	-47.86
Fe/LrGO[11]	1.9	20	-54.2
RGO-Fe$_3$O$_4$@ZnO[12]	5.0	30	-38.0
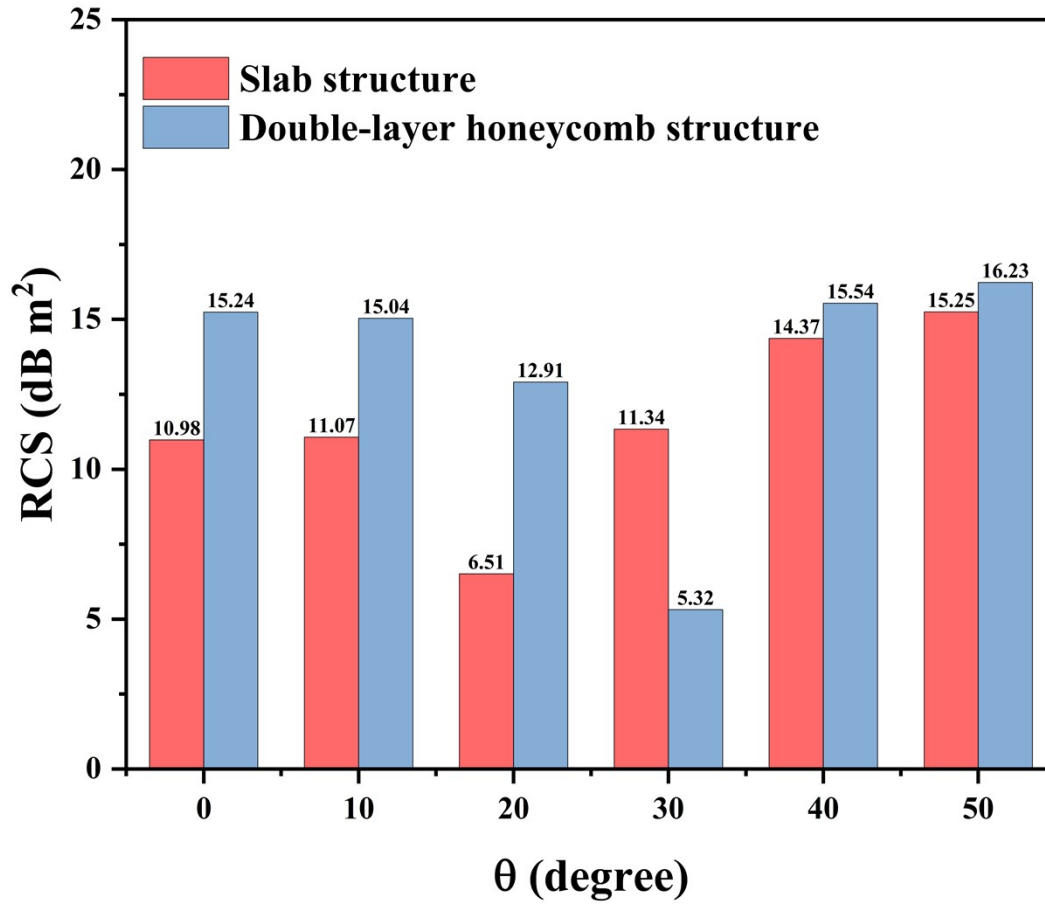
Fig. S5. RCS reduction values at representative scan angles.

Reference

1. P. Liu, S. Shi, Y. Ni, K. Xu, Q. Gao, Z. Hao, Z. Tian, W. Xiao, G. Xu and F. Liu, *Chem. Eng. J.*, 2023, **478**, 147474.

2. X. Ding, Y. Huang, S. Li, N. Zhang and J. Wang, *Compos. Pt. A-Appl. Sci. Manuf.*, 2016, **90**, 424-432.

3. H. Li, S. Bi, J. Cai, X. Chu, G. Hou, J. Zhang and T. Wu, *Carbon*, 2024, **223,** 119005.

4. Y. M. Li, Y. R. Li, H. P. Fang, Y. Deng and D. Y. Wang, *ACS Appl Mater Interfaces*, 2024, **16**, 51333-51345.

5. J. Su, X. Zhang, Z. Ma, X. Xu, J. Xu and Y. Chen, *Carbon*, 2024, **229,** 119448.

6. S. Wang, B. Wen, X. Liu, S. Xue, J. Xiao, L. Li, G. Yang and S. Ding, *Applied Materials Today*, 2024, **41,** 102461.

7. J. Xu, X. Xu, Z. Ma, X. Zhang, F. Yan, P. Yang, C. Zhu and Y. Chen, *Carbon*, 2024, **228,** 119409.

8. K. Zhang, Y. Liu, Y. Liu, Y. Yan, G. Ma, B. Zhong, R. Che and X. Huang, *Nanomicro Lett*, 2024, **16**, 66.

9. Q. Su, Y. He, D. Liu, D. Li, L. Xia, X. Huang and B. Zhong, *Nano Res.*, 2023, **17**, 1687-1698.

10. Y. Li, Y. Jin, J. Cheng, Y. Fu, J. Wang, L. Fan, D. Zhang, P. Zhang, G. Zheng and M. Cao, *Carbon*, 2023, **213,** 118245.

11. Y. Ge, H. Wang, T. Wu, B. Hu, Y. Shao and H. Lu, *J Colloid Interface Sci*, 2022, **628**, 1019-1030.

12. D. Sun, Q. Zou, Y. Wang, Y. Wang, W. Jiang and F. Li, *Nanoscale*, 2014, **6**, 6557-6562.